Journal of Solid Mechanics Vol. 4, No. 3 (2012) pp. 313-326

Semi-analytical Solution for Time-dependent Creep Analysis of Rotating Cylinders Made of Anisotropic Exponentially Graded Material (EGM)

A. Loghman[1,*], V. Atabakhshian[2]

[1]*Faculty of Mechanical Engineering, University of Kashan, Kashan, Iran*
[2]*Department of Mechanical Engineering, Faculty of Engineering, Bu-Ali Sina University, Hamedan, Iran*

Received 27 August 2012; accepted 5 October 2012

ABSTRACT

In the present paper, time dependent creep behavior of hollow circular rotating cylinders made of exponentially graded material (EGM) is investigated. Loading is composed of an internal pressure, a distributed temperature field due to steady state heat conduction with convective boundary condition and a centrifugal body force. All the material properties are assumed to be exponentially graded along radius. A semi analytical solution followed by the method of successive approximation has been developed to obtain history of stresses and deformations during creep evolution of the EGM rotating cylinder. The material creep constitutive model is defined by the Bailey-Norton time-dependent creep law. A comprehensive comparison has been made between creep response of homogenous and non-homogenous cylinder. It has been found that the material in-homogeneity exponent has a significant effect on creep response of the EGM cylinder. It has been concluded that using exponentially graded material significantly decreases creep strains, stresses and deformations of the EGM rotating cylinder.

Keywords: EGM Rotating cylinder; Bailey-Norton creep law; History of stresses

1 INTRODUCTION

FUNCTIONALLY graded materials (FGM) are used in modern technologies for structural components mostly used in nuclear power plants, aircraft industries, space engineering and pressure vessels. These materials are intentionally designed so that their properties are variable in the prescribed directions in space. Many investigators have used power law variation for material properties to analyze the structural components [1, 2]. Recently, exponential law for material properties attracted more attention due to offering useful and advantages characteristics by several authors [3,4]. Effects of material anisotropic properties on elastic and creep behavior of components have been an active area of research in the past decade. There have been some studies dealing with elastic and steady state creep analysis of FG rotating cylinders. Fukui and Yamanaka [5] investigated the effects of the material grading index on the strength and deformation of thick walled Functionally Graded (FG) tubes under internal pressure. Loghman and Wahab [6] studied the creep stress and damage histories of thick-walled tubes using the material constant creep and creep rupture properties defined by the "Theta Projection Concept" [7]. Loghman and Shokouhi [8] investigated creep stress redistribution and damage histories of thick-walled spheres using the same "Theta Projection Concept" for material properties. Aleayoub and Loghman [9] considered creep stress redistribution Analysis of thick-walled FGM spheres. Chen et al [10] studied the creep behavior of thick walled

* Corresponding author. Tel.: +98 361 5912425 ; Fax: +98 361 5559930.
E-mail address: aloghman@kashanu.ac.ir (A. Loghman).

cylinders made of FGM and subjected to both internal and external pressures. They obtained the asymptotic solutions on the basis of Taylor expansion series and compared it with the results of Finite Element analysis (FEA) obtained by using ABAQUS software. You et al [11] analyzed the steady state creep in thick walled cylinders made of arbitrary FGMs and subjected to internal pressure. Singh et al. [12] investigated effect of anisotropy on the steady state creep in functionally graded cylinder subjected to internal and external pressures. The subject of time-dependent creep analysis is considered by several investigators. Yang [13] and Xuan et al. [14]. Time-dependent Magneto-thermo-elastic creep analysis of functionally graded cylinders has been investigated by Loghman et al. [15]. Stress and deformation histories of FGM cylinders subjected to internal pressure, thermal and magnetic field are presented. In another study Loghman et al. [16] considered time-dependent magneto-thermo-elastic creep modeling of FGM spheres using method of successive elastic solution. Time-dependent creep stress redistribution analysis of thick-walled functionally graded spheres has been presented by Loghman et al. [17]. History of stresses and strains during creep evolution are reported. Time-dependent thermoelastic creep analysis of rotating disk made of Al–SiC composite has been carried out by Loghman et al. [18]. They have shown that time-dependent creep stress redistributions approaches the steady-state solution after almost 50 years.

The main objective of this paper is to study the time-dependent creep behavior of rotating cylinders made from exponentially graded material using Bailey-Norton creep constitutive model.

2 HEAT CONDUCTION PROBLEM WITH CONVECTIVE BOUNDARY CNDITION AT OUYER SURFACE

In this study, a distributed temperature field due to steady-state heat conduction with convective boundary condition at outer surface of the EGM cylinder has been considered. The geometry and thermo-mechanical loading and boundary conditions of the problem are shown in Fig. 1. The heat transfer equation in the cylindrical coordinate system is given by [19]

$$\frac{1}{r}\frac{\partial}{\partial r}\left[rK_T(r)\frac{\partial T(r)}{\partial r}\right]=0,\ (a\le r\le b). \tag{1}$$

The boundary conditions are considered as:

$$\begin{aligned} &T(r)=T_0 \quad at\ \ r=a,\\ &\left[\frac{\partial T(r)}{\partial r}+HT(r)\right]=0\ \ at\ \ r=b, \end{aligned} \tag{2}$$

where H is the ratio of convective heat transfer coefficient and $K_T(r)$ is the radial-dependent thermal conduction coefficient, which is assumed to be an exponential function of r as follows:

$$K_T(r)=k_0\exp\left[\beta\frac{r-a}{b-a}\right]. \tag{3}$$

Substituting Eq. (3) into the heat conduction Eq. (1), yields the general solution for the temperature distribution as follows:

$$T(r)=Z_1\,\mathrm{Ei}\left(1,\frac{r\beta}{b\text{-}a}\right)+Z_2, \tag{4}$$

where the exponential integral function, $\mathrm{Ei}(a,z)$, is defined for $\mathrm{Re}(z)>0$ by [20]

$$\mathrm{Ei}(a,z)=\int_1^{\infty}\frac{\exp(-tz)}{t^a}dt. \tag{5}$$

The unknowns, Z_1 and Z_2 are determined using boundary condition Eq. (2) as:

$$Z1 = \frac{HbT_0}{\exp(\frac{\beta b}{a-b}) - Hb\,\mathrm{Ei}\left(1, \frac{\beta b}{b-a}\right) + Hb\,\mathrm{Ei}\left(1, \frac{\beta a}{b-a}\right)},$$
$$Z2 = -\frac{T_0\left(-\exp\left(\frac{\beta b}{a-b}\right) + Hb\,\mathrm{Ei}\left(1, \frac{\beta b}{b-a}\right)\right)}{\exp(\frac{\beta b}{a-b}) - Hb\,\mathrm{Ei}\left(1, \frac{\beta b}{b-a}\right) + Hb\,\mathrm{Ei}\left(1, \frac{\beta a}{b-a}\right)}. \quad (6)$$

Temperature distribution and the effect of thermal in-homogeneity parameter β are illustrated in Fig. 2.

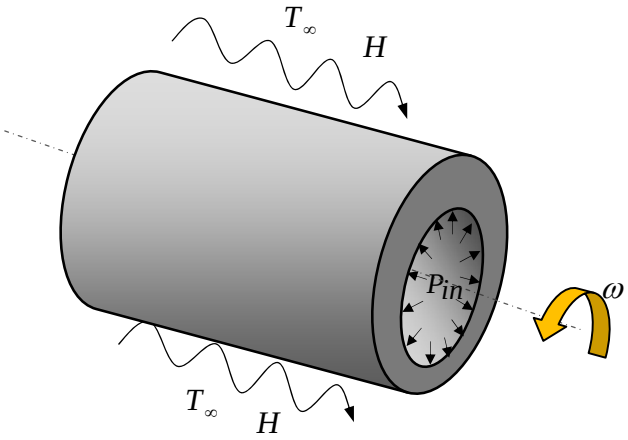

Fig. 1
Schematic of anisotropic exponentially graded material (EGM) rotating cylinder under thermo mechanical loadings.

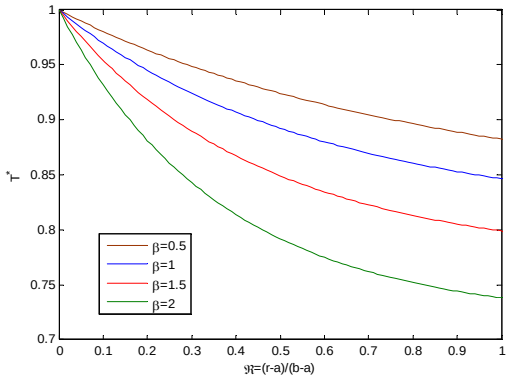

Fig. 2
Distribution of dimensionless temperature versus dimensionless radial coordinates for variable thermal in-homogeneity parameter.

3 BASIC FORMULATION

Consider a long rotating EGM cylinder subjected to an internal pressure and the above mentioned temperature distribution. Assuming total strains to be the sum of elastic, thermal and creep strains and employing the plain-strain assumption the stress-strain relations in terms of displacement, thermal and creep strains are written as follows:

$$\sigma_{rr} = C_{11}\frac{\partial u}{\partial r} + C_{12}\frac{u}{r} - \lambda_1 T(r) - \gamma_1 \varepsilon_{rr}^{C},$$
$$\sigma_{\theta\theta} = C_{12}\frac{\partial u}{\partial r} + C_{22}\frac{u}{r} - \lambda_2 T(r) - \gamma_2 \varepsilon_{\theta\theta}^{C}, \quad (7)$$

where

$$\lambda_1 = C_{11}\alpha_r + C_{12}(\alpha_\theta + \alpha_z), \lambda_2 = C_{11}\alpha_\theta + C_{12}(\alpha_r + \alpha_z). \tag{8}$$

In this study, we want to describe useful and advantages impression of exponentially graded material property on history of stresses and deformations due to creep phenomenon. Hence, material in-homogeneity property used in this study is taken as follows:

$$\Psi_r = \Psi_0 \exp\left(\mu \frac{r-a}{b-a}\right). \tag{9}$$

where Ψ_r represents the general material properties of the cylinder such as elastic parameters, thermal expansion coefficients, creep strain coefficients and mass density, and Ψ_0 corresponds to the value of the coefficients at the inner surface.

The equilibrium equation of rotating cylinder is given by:

$$\frac{\partial \sigma_{rr}}{\partial r} + \frac{\sigma_{rr} - \sigma_{\theta\theta}}{r} + \rho r \omega^2 = 0. \tag{10}$$

Substituting Eq. (7) into Eq. (10) yields the following constitutive differential equation with variable and time-dependent coefficients as:

$$\begin{aligned} &\frac{d^2u(r)}{dr^2} + D_1(r)\frac{du(r)}{dr} + D_2(r)u(r) = \\ &D_3(r)\varepsilon_{rr}^C + D_4(r)\varepsilon_{\theta\theta}^C + D_5(r)\frac{d\varepsilon_{rr}^C}{dr} + D_6(r)T(r) + D_7(r)\frac{dT(r)}{dr} + D_8(r), \end{aligned} \tag{11}$$

where the variable coefficients are:

$$\begin{aligned} &D_1(r) = \frac{1}{C_{11}(r)}\left(\frac{dC_{11}(r)}{dr}\right) + \frac{1}{r}; D_2(r) = \frac{1}{r^2 C_{11}(r)}\left(\frac{dC_{12}(r)}{dr} r - C_{22}(r)\right); \\ &D_3(r) = \frac{1}{C_{11}(r)}\left(\frac{d\gamma_1(r)}{dr} + \frac{\gamma_1(r)}{r}\right); D_4(r) = -\frac{\gamma_2(r)}{rC_{11}(r)}; \\ &D_5(r) = \frac{\gamma_1(r)}{C_{11}(r)}; D_6(r) = \frac{1}{C_{11}(r)}\left(\frac{d\lambda_1(r)}{dr} + \frac{\left(\lambda_1(r) - \lambda_2(r)\right)}{r}\right); \\ &D_7(r) = \frac{\lambda_1(r)}{C_{11}(r)}; \quad D_8(r) = -\frac{\rho r \omega^2}{C_{11}(r)}; \end{aligned} \tag{12}$$

No exact solution for Eq. (11) can be obtained, since its right hand side contains functions of time-dependent creep strains and existing exponential in-homogeneity parameters (i.e. Eq. (9)). Hence, a semi-analytical method has been employed to solve it as discussed below.

4 SOLUTION ALGORITHMS

4.1 Semi-analytical method

A semi-analytical method for solution of the differential Eq. (11) has been applied. The solution domain is first divided into some finite divisions [21, 18]. The coefficients of Eq. (11) are evaluated at r^m, mean radius of mth

division, and therefore, the differential equation with constant coefficients become valid only for the mth sub-domain which can be re-written as [21]

$$\left(P_1^m \frac{d^2}{dr^2} + P_2^m \frac{d}{dr} + P_3^m\right) u^m + P_4^m = 0 \tag{13}$$

where

$$\begin{aligned}
P_1^m &= C_{11}(r^m);\\
P_2^m &= \left.\frac{dC_{11}(r)}{dr}\right|_{r=r^m} + \frac{C_{11}(r^m)}{r^m};\\
P_3^m &= \left.\frac{1}{r^m}\frac{dC_{12}(r)}{dr}\right|_{r=r^m} - \frac{C_{22}(r^m)}{r^{m2}};\\
P_4^m &= -\left(\left.\frac{d\gamma_1(r)}{dr}\right|_{r=r^m} + \frac{\gamma_1(r^m)}{r^m}\right)\varepsilon_{rr}^C\Big|_{r=r^m} + \frac{\gamma_2(r^m)}{r^m}\varepsilon_{\theta\theta}^C\Big|_{r=r^m}\\
&\quad - \gamma_1(r^m)\left.\frac{d\varepsilon_{rr}^C}{dr}\right|_{r=r^m} + Z_1\left(\frac{\lambda_2(r^m)-\lambda_1(r^m)}{r^m} - \left.\frac{d\lambda_1(r)}{dr}\right|_{r=r^m}\right)\mathrm{Ei}\left(1, \frac{\beta r^m}{b-a}\right)\\
&\quad + \frac{\lambda_1(r^m)Z_1}{r^m}\exp\left(\frac{\beta r^m}{a-b}\right) - Z_2\left.\frac{d\lambda_1(r)}{dr}\right|_{r=r^m} + Z_2\frac{\lambda_2(r^m)-\lambda_1(r^m)}{r^m} + \rho(r^m)r^m\omega^2;
\end{aligned} \tag{14}$$

The coefficients of Eq. (13) are evaluated in each division in terms of geometric and material constants and the radius of mth division. Hence, the differential equation can now be solved since the terms corresponding to the creep strain functions on the right hand side of the equation have become known. The general solution for Eq. (13) in terms of unknown constants (X_1^m, X_2^m) could be written as follows:

$$u^m = X_1^m \exp(\xi_1^m r) + X_2^m \exp(\xi_2^m r) - \frac{P_4^m}{P_3^m} \quad , \quad r^m - \frac{h^m}{2} \le r \le r^m + \frac{h^m}{2} \tag{15}$$

where

$$\xi_{\mathrm{I}}^m, \xi_{\mathrm{2}}^m = -\frac{P_2^m \pm \sqrt{P_2^{m2} - 4P_3^m P_1^m}}{2P_1^m}, \tag{16}$$

Substituting the displacement from Eq. (15) into Eq. (7), the radial and circumferential stresses are evaluated. Subsequently, the unknowns X_1^m and X_2^m are determined by applying the necessary boundary conditions between two adjacent sub-domains. For this purpose, the continuity of the radial displacement u as well as radial stress σ_r are imposed at the interfaces of the adjacent sub-domains as follows:

$$u^m\Big|_{r=r^m+\frac{h^m}{2}} = u^{m+1}\Big|_{r=r^m-\frac{h^m}{2}}$$
$$\sigma_{rr}^m\Big|_{r=r^m+\frac{h^m}{2}} = \sigma_{rr}^{m+1}\Big|_{r=r^m-\frac{h^m}{2}} \tag{17}$$

The global boundary conditions at inner and outer surfaces of the hollow cylinder expressed as:

$$\sigma_{rr}\Big|_{r=a} = -P_{in} \quad , \quad \sigma_{rr}\Big|_{r=b} = 0 \tag{18}$$

The continuity conditions Eq. (17) together with the global boundary conditions (18) yields a set of linear algebraic equations in terms of X_1^k and X_2^k. Solving the resultant linear algebraic equations, the unknown coefficients are calculated. Then, the displacement component and radial and circumferential stresses are determined in each radial sub-domain. Increasing the number of divisions improves the accuracy of the results.

4.2 Time dependent creep analyses

Creep strain rates are related to the stresses and the material uniaxial creep constitutive model by the well known Prandtle-Reuss equations as:

$$\dot{\varepsilon}_{rr}^C = \frac{\dot{\varepsilon}_e^C}{\sigma_e}\left[\sigma_{rr} - 0.5\left(\sigma_{\theta\theta} + \sigma_{zz}\right)\right], \tag{19}$$

$$\dot{\varepsilon}_{\theta\theta}^C = \frac{\dot{\varepsilon}_e^C}{\sigma_e}\left[\sigma_{zz} - 0.5\left(\sigma_{zz} + \sigma_{rr}\right)\right], \tag{20}$$

$$\dot{\varepsilon}_{zz}^C = \frac{\dot{\varepsilon}_e^C}{\sigma_e}\left[\sigma_{zz} - 0.5\left(\sigma_{rr} + \sigma_{\theta\theta}\right)\right]. \tag{21}$$

For plane-strain condition the axial creep strain rate disappears (i.e. $\dot{\varepsilon}_{zz}^C = 0$) and from Eq. (21) the axial stress can be written as follows:

$$\sigma_{zz} = 0.5\left(\sigma_{\theta\theta} + \sigma_{rr}\right). \tag{22}$$

Substituting Eq. (22) into Eqs. (19) and (20) the radial and circumferential strain rates are evaluated as:

$$\dot{\varepsilon}_{rr}^C = \frac{3\dot{\varepsilon}_e^C}{4\sigma_e}\left(\sigma_{rr} - \sigma_{\theta\theta}\right), \tag{23}$$

$$\dot{\varepsilon}_{\theta\theta}^C = \frac{3\dot{\varepsilon}_e^C}{4\sigma_e}\left(\sigma_{\theta\theta} - \sigma_{rr}\right). \tag{24}$$

The Bailey–Norton's creep constitutive model for the effective strain is [22]

$$\dot{\varepsilon}_e^C = B(r)t^q\,\sigma_e^{n(r)}, \tag{25}$$

where $B(r)$ and $n(r)$ are the radial-dependent material creep parameters and q is a constant coefficient which $1/3 \le q \le 1/2.$. In this study $B(r) = b_0 r^{b_1}$ and $n(r)$ is considered to be a constant $n(r) = n_0$.

Considering the Von Mises equivalent stress

$$\sigma_e = \frac{1}{\sqrt{2}} \sqrt{\left(\sigma_{\theta\theta} - \sigma_{rr}\right)^2 + \left(\sigma_{\theta\theta} - \sigma_{zz}\right)^2 + \left(\sigma_{zz} - \sigma_{rr}\right)^2} \tag{26}$$

and substituting Eq. (22) into Eq. (26) the effective stress may be reduced as:

$$\sigma_e = \frac{\sqrt{3}}{2}\left(\sigma_{\theta\theta} - \sigma_{rr}\right) \tag{27}$$

4.3 Successive approximation method to obtain history of creep stresses

A successive approximation method has been employed to obtain history of creep stresses, strains and deformation as follows:

1. Assuming an appropriate time increment at each timing step. The total time is therefore the sum of time increments during the progress of the creep process. For the ith timing step, the total time is $t_i = \sum_{k=1}^{i-1} \Delta t_k + \Delta t_i$.

2. Estimating creep strain increments in radial and circumferential directions at any division point and any timing step. Hence, the same initial estimates at all divisions are considered (as $\Delta\varepsilon_{rr}^{C} = -0.00001$ and $\Delta\varepsilon_{\theta\theta}^{C} = 0.00001$). Creep strain at any point throughout the thickness of the cylinder is the cumulative sum of all previous creep strains as:

$$\begin{aligned} \varepsilon_{rr,im}^{C} &= \sum_{k=1}^{i-1} \Delta\varepsilon_{rr,km}^{C} + \Delta\varepsilon_{rr,im}^{C}, \\ \varepsilon_{\theta\theta,im}^{C} &= \sum_{k=1}^{i-1} \Delta\varepsilon_{\theta\theta,km}^{C} + \Delta\varepsilon_{\theta\theta,im}^{C}, \end{aligned} \tag{28}$$

where the subscripts i and m indicate the timing steps and division points, respectively.

3. First order derivative of radial creep strain are calculated using finite difference approximation as follows:

$$\frac{d\varepsilon_{rr,im}^{C}}{dr} = \frac{\varepsilon_{rr,im+1}^{C} - \varepsilon_{rr,im-1}^{C}}{2h} \tag{29}$$

4. Cumulative creep strains and its first order derivatives are substituted in Eq. (13). This differential equation can be solved for the displacement at mth layer. Using local and global boundary conditions the displacements at time t_i are determined. Furthermore, substituting resultant radial displacement in Eq. (7), component of radial and circumferential stresses for each division points are achieved.

5. Substituting radial and circumferential stresses from step 4 in Eq. (27), effective stresses are evaluated for each division.

6. Effective creep strain rates are then calculated at all division points (m) for ith timing step using Bailey–Norton's creep constitutive model using Eq. (25).

7. From Prandtl–Reuss relation, radial and circumferential creep strain rates are obtained Eq. (23) and Eq. (24).

8. New values for radial and circumferential creep strain increments at all division points are obtained using the above creep strain rates (stage 7) and the time increment.

$$\Delta\varepsilon_{rr,im}^{C,new} = \dot{\varepsilon}_{rr,im}^{C} \times \Delta t_i,$$
$$\Delta\varepsilon_{\theta\theta,im}^{C,new} = \dot{\varepsilon}_{\theta\theta,im}^{C} \times \Delta t_i. \quad (30)$$

9. These new obtained values for creep strain increments are compared with the estimated values and if needed replaced and the procedure is repeated until the required convergence is achieved. In the next time step, the first estimate for creep strain increments is the converged value obtained from the previous time step; hence, the procedure is continued from stage 2.

5 NUMERICAL RESULTS AND DISCUSSION

In this section an exponentially graded rotating cylinder is considered with radius ratio of $\frac{a}{b} = 0.5$ which is rotating with a constant angular velocity of $\omega = 400\, rad/s$. The internal pressure applied on the cylinder is $P_{in} = 2\, MPa$. The material parameters are $E = 22GPa$, $\rho_0 = 3000\, kg/m^3$, $\alpha_{r0} = 16.28e-6(1/K)$, $\alpha_{\theta 0} = \alpha_{z0} = 26.38e-6(1/K)$ and $\nu = 0.3$. The ratio of the convective heat transfer coefficient is 0.72. The Bailey–Norton's creep constitutive constants are $b_0 = 1e-28$, $b_1 = 1$, $q = 1/3$ and $n = 3$. Other elastic constants are obtained from the following relations $C_{110} = \frac{E(1-\nu)}{((1+\nu)(1-2\nu))}$, $C_{120} = \frac{E\nu}{((1+\nu)(1-2\nu))}$, $\gamma_0 = \frac{E}{(1+\nu)}$, and non-dimensional parameters introduced by $\Re = \frac{r-a}{b-a}, \sigma_{ii}^* = \frac{\sigma_{ii}}{P_{in}} (i = r, \theta), \sigma_z^* = \frac{\sigma_{zz}}{P_{in}}, \sigma_e^* = \frac{\sigma_e}{P_{in}}, U_r^* = \frac{u(r)}{a}$ and $T^* = \frac{T(r)}{T_{in}}$.

5.1 Example 1

To show the effect of in-homogeneity parameter on initial elastic stress response of the EGM cylinders the range of $-2 \le \mu \le 2$ are considered in this example. Considering $\varepsilon_{rr}^C = 0$ and $\varepsilon_{\theta\theta}^C = 0$, Eqs. (9) and (10) are reduced to elastic constitutive equations at zero time. Figs. 3-7 show the radial, circumferential, axial and effective stress distributions and radial displacement of EGM hollow rotating cylinder respectively. The temperature field of EGM hollow rotating cylinder due to steady state heat conduction with convective boundary condition at various thermal in-homogeneity exponents are presented in section 2. From the curve of Fig. 3, it is shown that the radial stresses satisfying the boundary conditions at the inner and outer surface of the EGM cylinder and are significantly affected by the in-homogeneity parameter μ. Figs. 4-6 show that the in-homogeneity parameter μ has also a great effect on the circumferential, axial and effective stresses. It is easily seen from Fig. 7 that increasing in-homogeneity parameter significantly decreases radial displacement throughout the thickness.

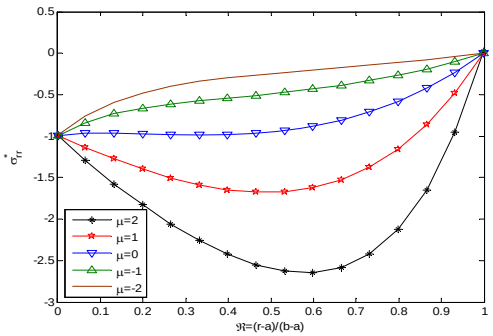

Fig. 3
Distribution of dimensionless radial stresses versus dimensionless radial coordinates with variable in-homogeneity parameter μ, and $\beta = 1$.

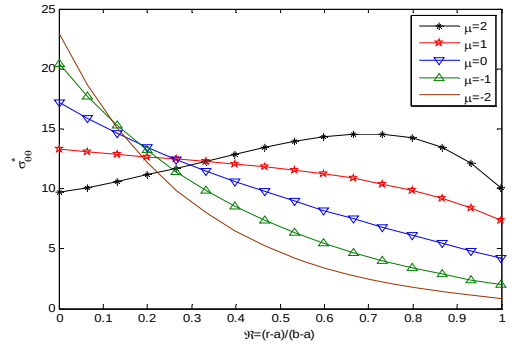

Fig. 4
Distribution of dimensionless circumferential stresses versus dimensionless radial coordinates with variable inhomogeneity parameter μ , and $\beta = 1$.

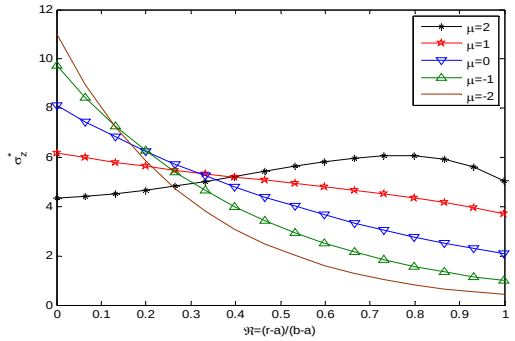

Fig. 5
Distribution of dimensionless axial stresses versus dimensionless radial coordinates with variable inhomogeneity parameter μ , and $\beta = 1$.

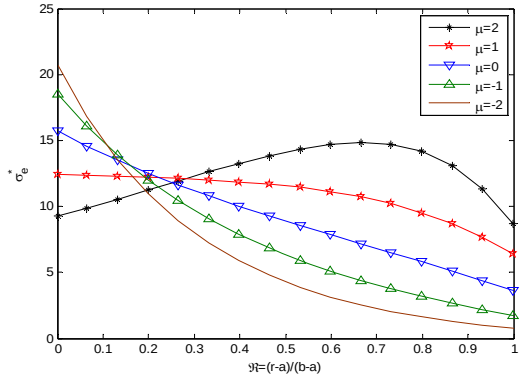

Fig. 6
Distribution of dimensionless effective stresses versus dimensionless radial coordinates with variable inhomogeneity parameter μ , and $\beta = 1$.

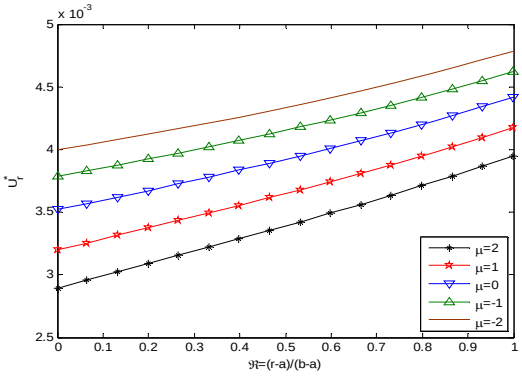

Fig. 7
Distribution of dimensionless radial displacement versus dimensionless radial coordinates with variable inhomogeneity parameter μ , and $\beta = 1$.

5.2 Example 2

For time dependent creep analyses the case of in-homogeneity parameter equal to $\mu = \beta = 1$ has been selected due to its most uniform effective stress distribution at zero time. History of stresses, strains and radial displacement from their initial elastic distribution at zero time up to 5 years are studied. In Figs. 8-14 results are presented for history of radial, circumferential, axial and effective stresses, radial displacement, radial and circumferential creep strains, respectively. In general radial, circumferential, axial and effective stresses are decreasing due to creep evolution as is evident from Figs. 8-11. The curves in Fig. 12 show maximum variation of normalized radial displacement after 5 years is not exceeded 1.2 percent of initial elastic case. Radial and circumferential creep strain histories are shown in Figs. 13 and 14. Due to incompressibility of material during creep evolution and the plane-strain condition of the problem the radial and circumferential creep strains are equal and opposite sign during creep process. In order to demonstrate the significant effect of exponentially law a homogeneous material is studied in example 3.

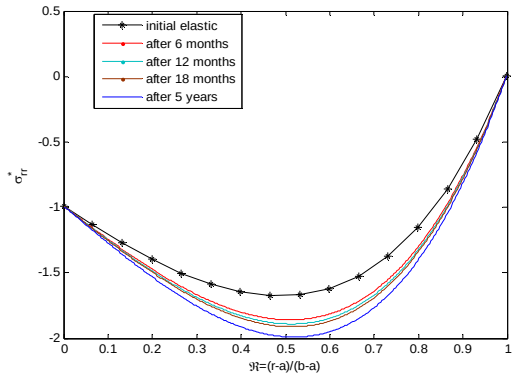

Fig. 8
History of dimensionless radial stresses from initial elastic up to 5 years for the case $\alpha = \beta = 1$.

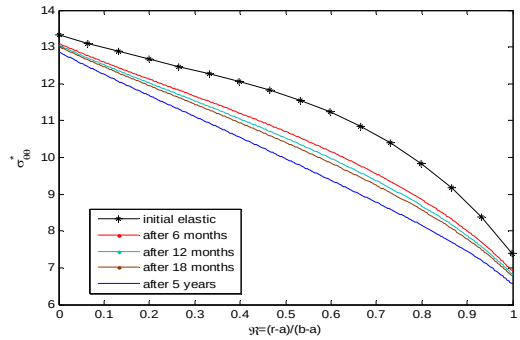

Fig. 9
History of dimensionless circumferential stresses from initial elastic up to 5 years for the case $\alpha = \beta = 1$.

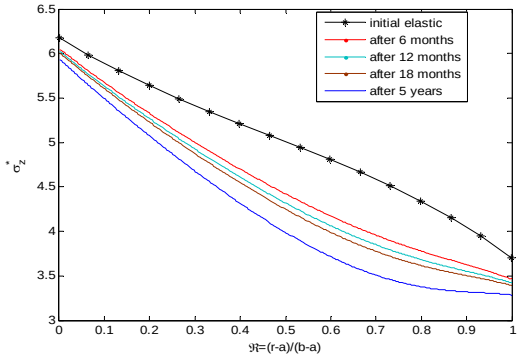

Fig. 10
History of dimensionless axial stresses from initial elastic up to 5 years for the case $\alpha = \beta = 1$.

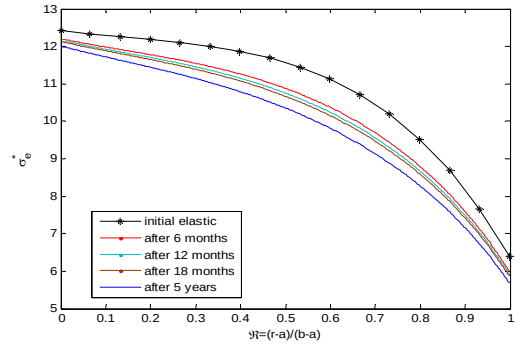

Fig. 11
History of dimensionless effective stresses from initial elastic up to 5 years for the case $\alpha = \beta = 1$.

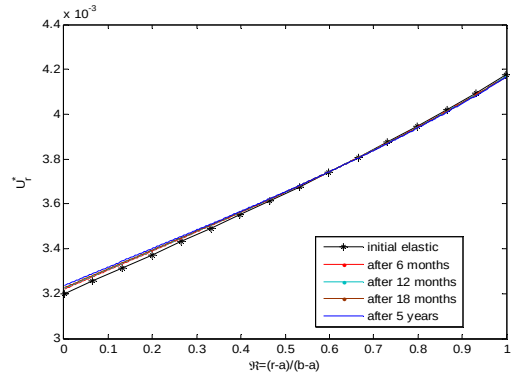

Fig. 12
History of dimensionless radial displacement from initial elastic up to 5 years for the case $\alpha = \beta = 1$.

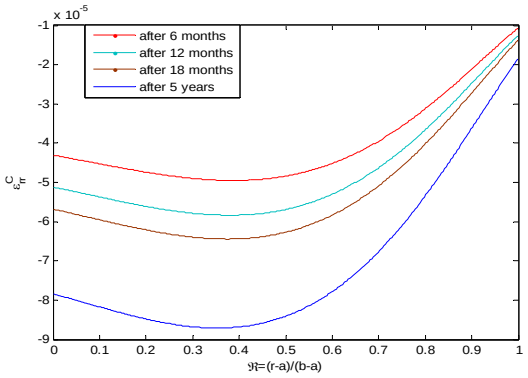

Fig. 13
History of radial creep strain from initial elastic up to 5 years for the case $\alpha = \beta = 1$.

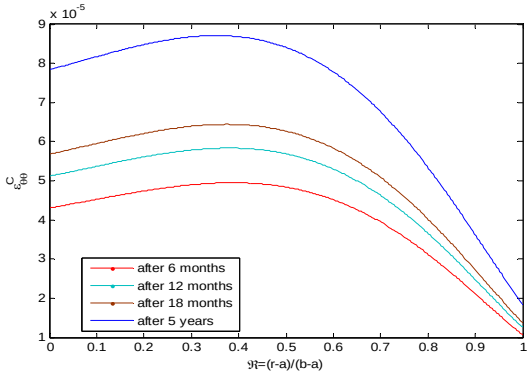

Fig. 14
History of circumferential creep strain from initial elastic up to 5 years for the case $\alpha = \beta = 1$.

5.3 Example 3

Setting the in-homogeneity exponent equal to zero ($\mu = \beta = 0$) a homogeneous material is considered to compare the results with an EGM defined by $\mu = \beta = 1$. The results are presented for history of radial, circumferential, axial and effective stresses, radial displacement, radial and circumferential creep strains in Figs. 15-21, respectively. Comparing history of stresses for homogeneous material depicted in Figs. 15-18 with EGM illustrated in Figs. 8-11 shows that exponential law for material property significantly decreases all stress levels at elastic and creep condition. The same conclusion can be reached comparing the radial displacement demonstrated in Fig 19. Creep strains in homogeneous material shown in Figs. 20-21are considerably higher than those in exponentially graded materials. This is an important and useful result for using exponentially graded materials.

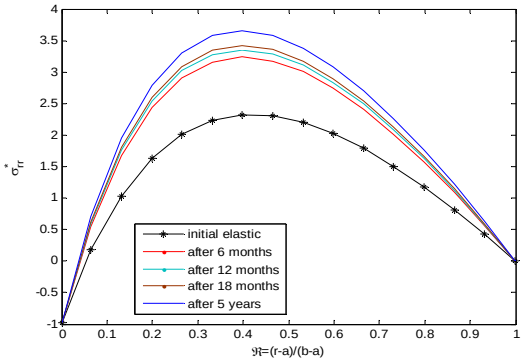

Fig. 15
History of dimensionless radial stresses from initial elastic up to 5 years for homogenous material $(\text{i.e. } \mu = \beta = 0)$.

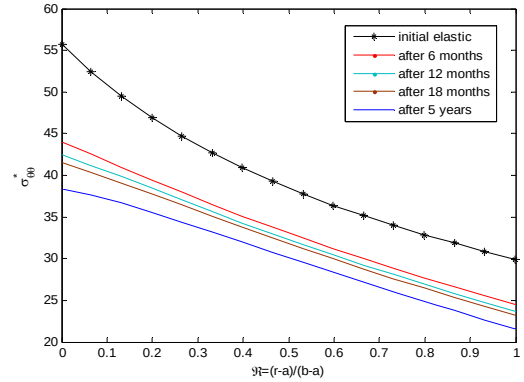

Fig. 16
History of dimensionless circumferential stresses from initial elastic up to 5 years for homogenous material $(\text{i.e. } \mu = \beta = 0)$.

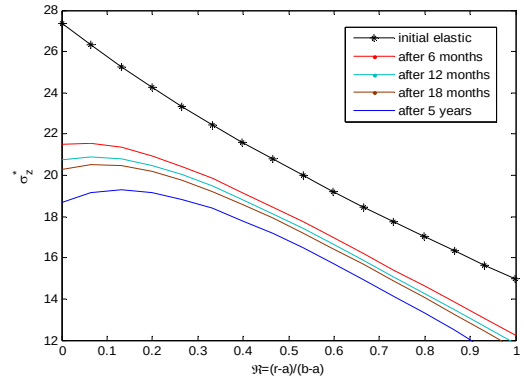

Fig. 17
History of dimensionless axial stresses from initial elastic up to 5 years for homogenous material $(\text{i.e. } \mu = \beta = 0)$.

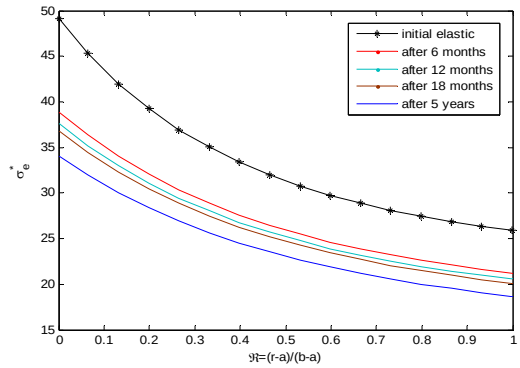

Fig. 18
History of dimensionless effective stresses from initial elastic up to 5 years for homogenous material $(\text{i.e. } \mu = \beta = 0)$.

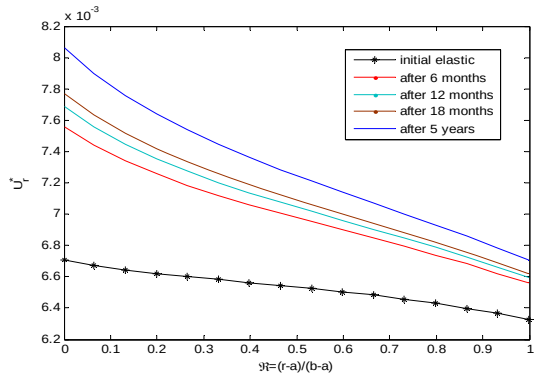

Fig. 19
History of dimensionless radial distribution from initial elastic up to 5 years for homogenous material $(\text{i.e. } \mu = \beta = 0)$.

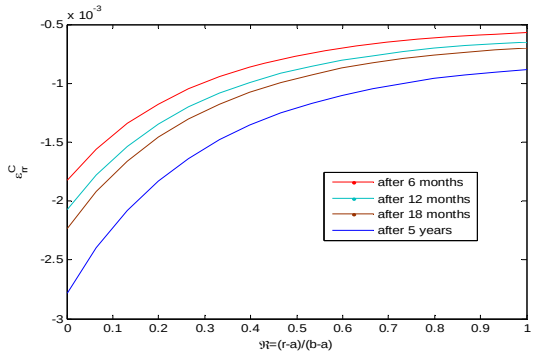

Fig. 20
History of radial creep strain from initial elastic up to 5 years for homogenous material $(\text{i.e. } \mu = \beta = 0)$.

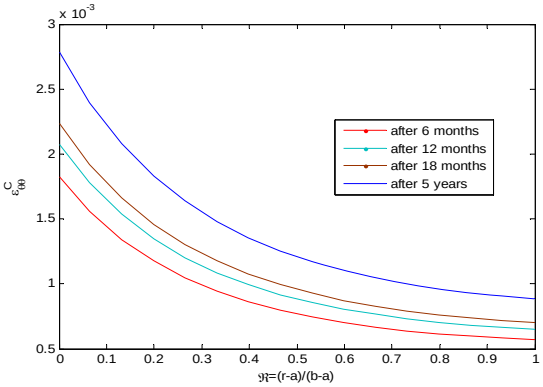

Fig. 21
History of circumferential creep strain from initial elastic up to 5 years for homogenous material $(\text{i.e. } \mu = \beta = 0)$.

6 CONCLUSIONS

From the results presented in this paper the following concluding remarks can be made:
1. Exponentially graded materials offered advantageous results to minimizing all thermo elastic and creep stresses. Hence, making EGM's is suggested for fabricating engineering structures which are subjected to high temperatures.
2. The material in-homogeneity parameter has a considerable effect on the thermoelastic and creep response of rotating cylinders made of EGMs.

ACKNOWLEDGEMENTS

The authors are grateful to University of Kashan for supporting this work by giving research grant No. 158467/2 to carry out this work.

REFERENCES

[1] Nie G.J., Batra R.C., 2010, Material tailoring and analysis of functionally graded isotropic and incompressible linear elastic hollow cylinders, *Composite Structures* **92** : 265–274.
[2] Bayat M., Sahari B.B., Saleem M., Ali A., Wong S.V., 2009, Bending analysis of a functionally graded rotating disk based on the first order shear deformation theory, *Applied Mathematical Modelling* **33** : 4215–4230.
[3] Ghorbanpour Arani A., Loghman A., Abdollahitaher A., Atabakhshian V., 2011, Electrothermomechanical behaviour of a radially polarized functionally graded piezoelectric cylinder, *Journal of Mechanics of Materials and Structures* **6** (6): 869–882.
[4] You L.H., Zhang J.J., You X.Y., 2005, Elastic analysis of internally pressurized thick-walled spherical pressure vessel of functionally graded materials, *International Journal of Pressure Vessels and Piping* **82**: 347–354.
[5] Fukui Y., Yamanaka N., 1992, Elastic analysis for thick-walled tubes of functionally graded material subjected to internal pressure, *JSME International Journal Series I* **35**: 379-385.
[6] Loghman A., Wahab M.A., 1996, Creep damage simulation of thick-walled tubes using the theta projection concept, *International Journal of Pressure Vessels and Piping* **67**: 105-111.
[7] Evans R.W., Parker J.D., Wilsher B., 1992, The theta projection concept a model based approach to design and life extention of engineering plant, *International Journal of Pressure Vessels and Piping* **50**: 60-147.
[8] Loghman A., Shokouhi N., 2009, Creep damage evaluation of thick-walled spheres using a long-term creep constitutive model, *Journal of Mechanical Science and Technology* **23**: 2577-2582.
[9] Aleayoub S.M.A., Loghman A., 2010, Creep stress redistribution Analysis of thick-walled FGM spheres, *Journal of solid Mechanics* **2** (2) :115-128.
[10] Chen J.J., Tu S.T., Xuan F.Z., Wang Z.D., 2007, Creep analysis for a functionally graded cylinder subjected to internal and external pressure, *The Journal of Strain Analysis Engineering Design* **42**: 69-77.
[11] You L.H., Ou H., Zheng Z.Y., 2007, Creep deformations and stresses in thick-walled cylindrical vessels of functionally graded materials subject to internal pressure, *Composite Structures* **78**:285-291.
[12] Singh T., Gupta V.K., 2011, Effect of anisotropy on steady state creep in functionally graded cylinder, *Composite Structures* **93**:747-758.
[13] Yang Y.Y., 2000, Time-dependent stress analysis in functionally graded material, *International Journal of Solids and Structures* **37**:7593-7608.
[14] Xuan F.Z., Chen J.J., Wang Z., Tu S.T., 2009, Time-dependent deformation and fracture of multi-material systems at high temperature, *International Journal of Pressure Vessels and Piping* **86**: 604-615.
[15] Loghman A., Ghorbanpour Arani A., Amir S., Vajedi A., 2010, Magnetothermoelastic creep analysis of functionally graded cylinders, *International Journal of Pressure Vessels and Piping* **87**:389-395.
[16] Loghman A., Aleayoub S.A.M., Hasani Sadi M., 2012, Time-dependent magnetothermoelastic creep Modeling of FGM spheres using method of successive elastic solution, *Applied Mathematical Modelling* **36**: 836-845.
[17] Loghman A., Ghorbanpour Arani A., Aleayoub S.A.M., 2011, Time-dependent creep stress redistribution analysis of functionally graded spheres, *Mechanics Time-Dependent Materials* **15:** 353-365.
[18] Loghman A., Ghorbanpour Arani A., Shajari A.R., Amir S., 2011, Time-dependent thermoelastic creep analysis of rotating disk made of Al–SiC composite, *Archive of Applied Mechanics* **81**:1853-1864.
[19] Hosseini SM., Akhlaghi M., Shakeri M., 2007, Transient heat conduction in functionally graded thick hollow cylinders by analytical method, *International Journal of Heat and Mass Transfer* **43**: 669-675.
[20] Abramowitz M., Stegun I., 1965, *Handbook of Mathematical Functions*, New York: Dover Publications Inc.
[21] Hosseini Kordkheili S.A., Naghdabadi R., 2007, Thermo-elastic analysis of a functionally graded rotating disk, *Composite Structures* **79**: 508-516.
[22] Penny RK., Marriott DL., 1995, *Design for creep*, London, Chapman & Hall.